

Perfect and robust phase-locking of a spin transfer vortex nano-oscillator to an external microwave source

A. Hamadeh,¹ N. Locatelli,² V. V. Naletov,^{1,2,3} R. Lebrun,² G. de Loubens,^{1,a)} J. Grollier,² O. Klein,¹ and V. Cros²

¹*Service de Physique de l'État Condensé (CNRS URA 2464), CEA Saclay, 91191 Gif-sur-Yvette, France*

²*Unité Mixte de Physique CNRS/Thales and Université Paris Sud 11, 1 av. Fresnel, 91767 Palaiseau, France*

³*Institute of Physics, Kazan Federal University, Kazan 420008, Russian Federation*

(Received 27 November 2013; accepted 3 January 2014; published online 16 January 2014)

We study the synchronization of the auto-oscillation signal generated by the spin transfer driven dynamics of two coupled vortices in a spin-valve nanopillar to an external source. Phase-locking to the microwave field h_{rf} occurs in a range larger than 10% of the oscillator frequency for drive amplitudes of only a few Oersteds. Using synchronization at the double frequency, the generation linewidth is found to decrease by more than five orders of magnitude in the phase-locked regime (down to 1 Hz, limited by the resolution bandwidth of the spectrum analyzer) in comparison to the free running regime (140 kHz). This perfect phase-locking holds for frequency detuning as large as 2 MHz, which proves its robustness. We also analyze how the free running spectral linewidth impacts the main characteristics of the synchronization regime. © 2014 AIP Publishing LLC. [<http://dx.doi.org/10.1063/1.4862326>]

Spin transfer nano-oscillators (STNOs) are nanoscale microwave generators^{1,2} which have become very attractive due to their wide range of potential applications (frequency generation^{3,4} and detection,^{5,6} signal processing,^{7,8} and dynamic recording^{9,10}). The transfer of angular momentum from a spin-polarized current to a ferromagnetic layer can excite the gyrotropic mode of a magnetic vortex,^{11,12} having typical frequency between 20 MHz and 2 GHz.¹³ Vortex-based STNOs are very promising due to their narrow generation linewidth (about 1 MHz) and potentially high output power.¹⁴ Recently, we have proposed a way to minimize even more the auto-oscillation linewidth by operating a STNO based on two coupled vortices in a spin-valve nanopillar, which can yield highly coherent signals ($Q > 15000$) with linewidths under 50 kHz at room temperature and near zero magnetic field.¹⁵

Synchronization to an external periodic signal and mutual phase-locking of several STNOs have been proposed as means to increase the emitted power and reduce the phase noise of STNOs.¹⁶ It has also been suggested that synchronized arrays of STNOs could be operated as associative memories.¹⁷ So far, mutual phase-locking has been achieved using spin wave coupling between nanocontacts^{18–20} and 2D arrays of vortices and anti-vortices.²¹ It is also predicted to occur using the common microwave current emitted^{22,23} or the dipolar interaction between adjacent STNOs.^{24,25} To demonstrate the efficiency of these two types of coupling, synchronization to an external microwave current passing through the device^{26–29} or to a microwave field produced by an external antenna^{30,31} have been studied.

Two key characteristics to analyze the quality of the synchronization are the locking range and the generation linewidth in the phase-locked regime, which are, respectively, related to the coupling efficiency and the response to noise of the oscillator. In a single vortex-based tunneling

magnetoresistance (TMR) device, it was shown that using an external microwave current, the locking range could reach up to one third of the oscillator frequency, and the linewidth be reduced by 3 orders of magnitude, from a few MHz down to 3 kHz.²⁹ In this Letter, we demonstrate perfect and robust synchronization of the microwave signal generated by the dynamics of two coupled vortices in a spin-valve nanopillar to an external microwave field h_{rf} . The linewidth measured in the phase-locked regime is indeed limited by the minimal resolution bandwidth (RBW) of the spectrum analyzer, which is 1 Hz. We observe such outstanding characteristics even for frequency detunings larger than ten times the free running linewidth (140 kHz).

The studied STNO is a circular nanopillar of diameter 250 nm patterned from a (Cu60|Py15|Cu10|Py4|Au25) stack, where thicknesses are in nm and Py = Ni₈₀Fe₂₀. An insulating resist is deposited onto the STNO device, and an external antenna is patterned on top to generate a spatially uniform microwave magnetic field h_{rf} oriented in the plane of the magnetic layers.³² By injecting a current $I_{dc} > 0$ through the STNO (electrons flowing from the thick to the thin Py layer), a vortex with chirality parallel to the orthoradial Oersted field is stabilized in each of the Py layers.^{15,33} A magnetic field H is applied perpendicularly to the sample plane and the vortex core polarities are set to be anti-parallel (see inset of Fig. 1(b)). For $I_{dc} \geq 10$ mA, a narrow microwave emission peak corresponding to the spin transfer driven dynamics of the two coupled vortices is detected on the spectrum analyzer.^{15,34} At fixed I_{dc} , the microwave characteristics of this auto-oscillation peak (frequency and linewidth) can be tuned by varying H .³⁵ In this study, all measurements are carried out at room temperature.

The perpendicular field is first set to $H_0 = 1$ kOe and the dc current fixed to $I_{dc} = 15$ mA. Under these bias conditions, the oscillator frequency is $F_0 = 586$ MHz and the generation linewidth $\Delta F_0 = 142$ kHz. In Fig. 1(a), we present a map of the power density when the frequency F_s of the external

^{a)}Electronic mail: gregoire.deloubens@cea.fr

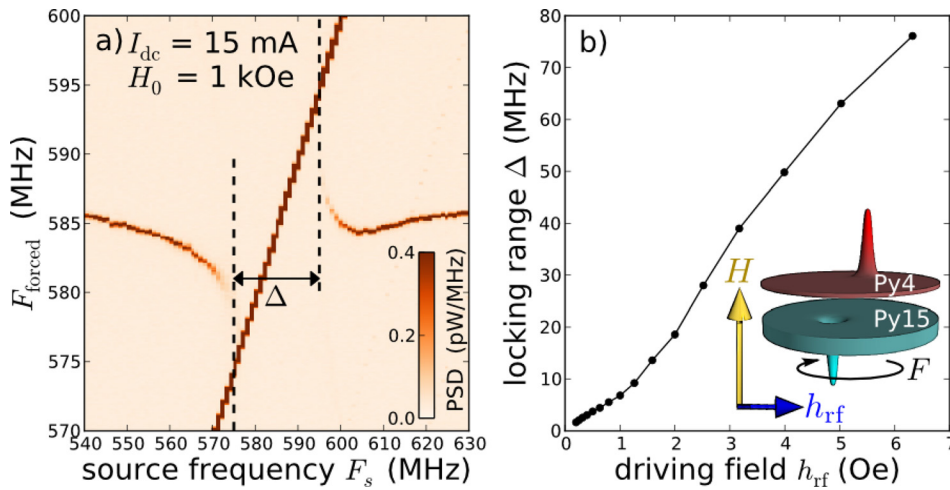


FIG. 1. (a) Power spectrum map of the STNO at $I_{dc} = 15$ mA and $H_0 = 1$ kOe vs. the frequency F_s of the external microwave field $h_{rf} = 2$ Oe. (b) Locking range Δ as a function of the drive amplitude.

microwave field is swept from 540 MHz to 630 MHz at constant drive amplitude $h_{rf} = 2$ Oe.³⁶ When F_s comes closer to F_0 , the frequency of the oscillator is pulled towards the source frequency. When $F_s \simeq 574$ MHz, there is a single frequency peak in the spectrum, meaning that the auto-oscillation is synchronized to the external source. At this point, it is not possible to separate the signal of the gyro-tropic oscillation and that of the source, which prevents measuring the generation linewidth in the phase-locked regime. This situation is observed until $F_s \simeq 597$ MHz, above which the oscillation frequency gradually shifts back to its free running value F_0 . The locking range Δ measured experimentally is plotted vs. h_{rf} in Fig. 1(b). As expected,¹⁶ it increases linearly with h_{rf} at low drive amplitude ($h_{rf} < 1.5$ Oe). The behavior observed at larger h_{rf} is presumably due to some nonlinearities of the system. We point out that at $h_{rf} = 6.3$ Oe, the locking range $\Delta = 75$ MHz corresponds to 13% of the oscillator frequency F_0 .

In order to measure the linewidth of the oscillator signal when its frequency is locked, the source frequency F_s is now swept around $2F_0$. In Fig. 2(a), we plot the frequency shift $F_{forced} - F_0$ of the oscillator when it is forced by the microwave field of amplitude $h_{rf} = 6.3$ Oe as a function of F_s varying from 1150 MHz to 1190 MHz. As in Fig. 1(a), we observe the characteristic behavior of synchronization to the external source, except that it is now at twice the oscillator frequency and the oscillation signal is not hindered by the source signal. Hence, we can analyze the dependence of the generation linewidth on F_s , which is plotted in Fig. 2(b). The striking observation is a dramatic reduction of the generation linewidth within the locking range. As shown in the inset of Fig. 2(b), the measured linewidth is indeed limited by the 1 Hz minimal RBW of the spectrum analyzer, i.e., the auto-oscillation is perfectly phase-locked to the external source. This corresponds to an improvement of the signal coherency by a factor greater than 10^5 with respect to the free running case. The increase of the generation linewidth up to 1 MHz observed at the boundaries of the locking range is attributed to successive synchronization-unsynchronization events, occurring at the timescale of the measurement.²⁹

To gain further insight, we investigate the robustness of this perfect phase-locking. We now measure the auto-oscillation signal as a function of I_{dc} , which is swept from 14.6 mA to 15.6 mA. In the free regime (external source

turned off), the generation frequency increases linearly from 584 MHz to 592 MHz, while the linewidth is nearly constant around $\Delta F_0 = 142$ kHz, as shown by the black dots in Figs. 3(a) and 3(b), respectively. The tunability observed in our vortex-based STNO, $dF_0/dI_{dc} \simeq 8$ MHz/mA, results from the Oersted field created by the dc current.³⁷ In the forced regime with the external source turned on at $F_s = 1175$ MHz and $h_{rf} = 6.3$ Oe (see blue dots in Fig. 3(a)), the auto-oscillation frequency is pulled towards half the source frequency $F_s/2$ for $I_{dc} < 14.9$ mA and $I_{dc} > 15.4$ mA, and constant and equal to $F_s/2$ in between these boundaries, which define the locking range. The associated decrease of the generation linewidth is spectacular, as shown by the logarithmic scale in Fig. 3(b). The measured linewidth is limited by the $RBW = 1$ Hz for $14.93 < I_{dc} < 15.35$ mA, which means that the phase-locking to the external source is perfect within this range of current. The latter corresponds to a variation by 4 MHz of the auto-oscillation frequency in the free

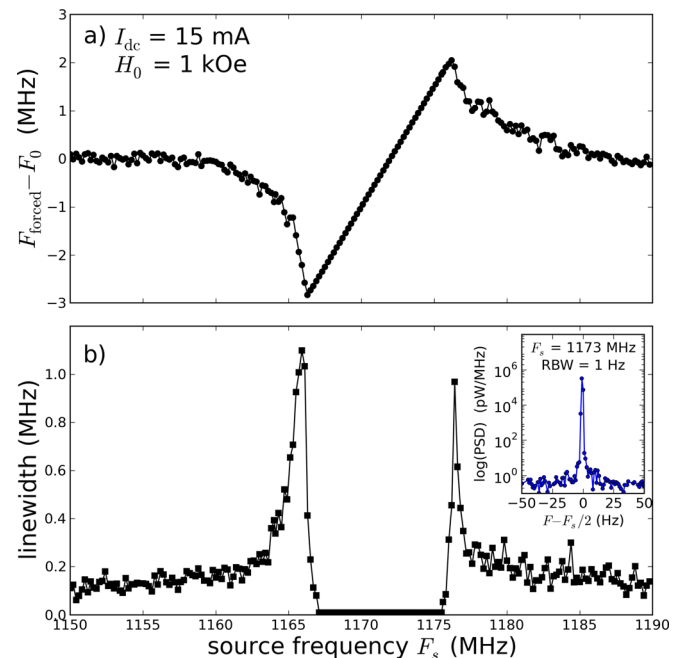


FIG. 2. (a) Frequency shift $F_{forced} - F_0$ and (b) linewidth of the generated signal as a function of the frequency of the source ($h_{rf} = 6.3$ Oe), swept around $2F_0$. The inset displays a measurement in the locking range (spectrum analyzer $RBW = 1$ Hz, frequency span = 100 Hz, sweep time = 2.3 s).

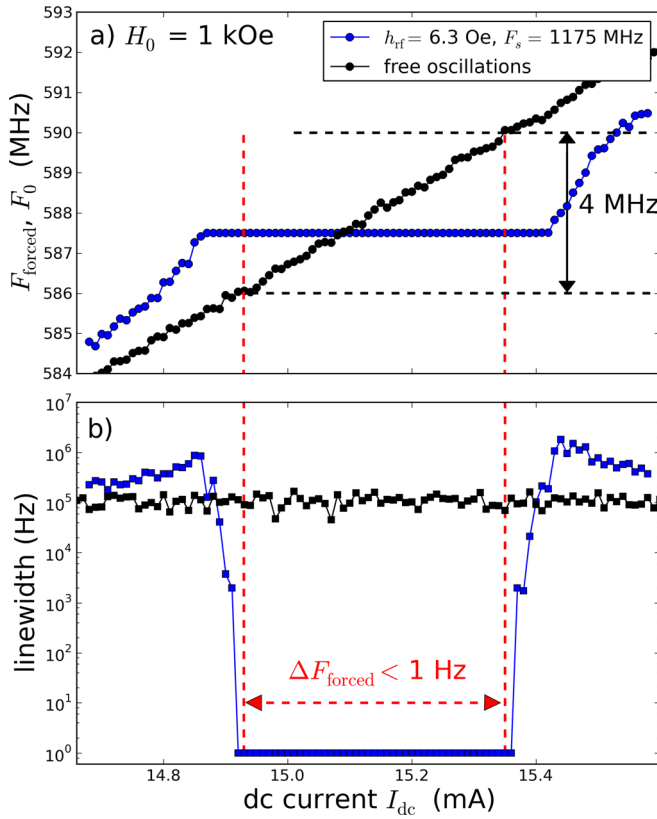


FIG. 3. Current dependence of the (a) STNO frequency and (b) generation linewidth in the free (black dots) and forced regimes (blue dots).

regime. These features demonstrate the robustness of the synchronization observed in our sample, as it means that even if the external source frequency deviates from the oscillator frequency by more than ten times the free running linewidth, perfect phase-locking can still occur.

Another issue to investigate is the influence of fluctuations³⁸ on the actual characteristics of our vortex oscillator when it is phase-locked. To do that, we compare the synchronization of auto-oscillation signals, having different generation linewidths. We use two different applied fields, $H_0 = +1$ kOe and $H_1 = -0.27$ kOe, at which the emission frequencies at $I_{dc} = 15$ mA slightly differ ($F_0 = 586$ MHz and $F_1 = 684$ MHz, respectively), and the generation linewidth varies by more than a factor seven,³⁹ from $\Delta F_0 = 142$ kHz to $\Delta F_1 = 1.05$ MHz (see inset of Fig. 4(a)). Using blue and red dots at H_0 and H_1 , respectively, we plot the experimental frequency mismatch $F_{\text{forced}} - F_s/2$ (Fig. 4(a)) and the linewidth in the forced regime (Fig. 4(b)) as a function of the detuning $F_{0,1} - F_s/2$ between the natural oscillator frequency and half the source frequency.⁴⁰ The strong differences observed in the characteristics of the synchronization at these two fields reveal the role played by the fluctuations in the phase dynamics of STNOs. When the latter are weak (narrower generation linewidth at H_0), the locking range is large (more than 4 MHz) and the synchronized signal acquires the spectral quality of the source (less than 1 Hz). When the noise is larger (broader generation linewidth at H_1), it competes against the coupling to the external source, which results in a smaller apparent locking range and a poorest spectral quality of the forced oscillation. Here, increasing the linewidth by a factor $\Delta F_1/\Delta F_0 \approx 7$ has a huge influence on the signal coherency in

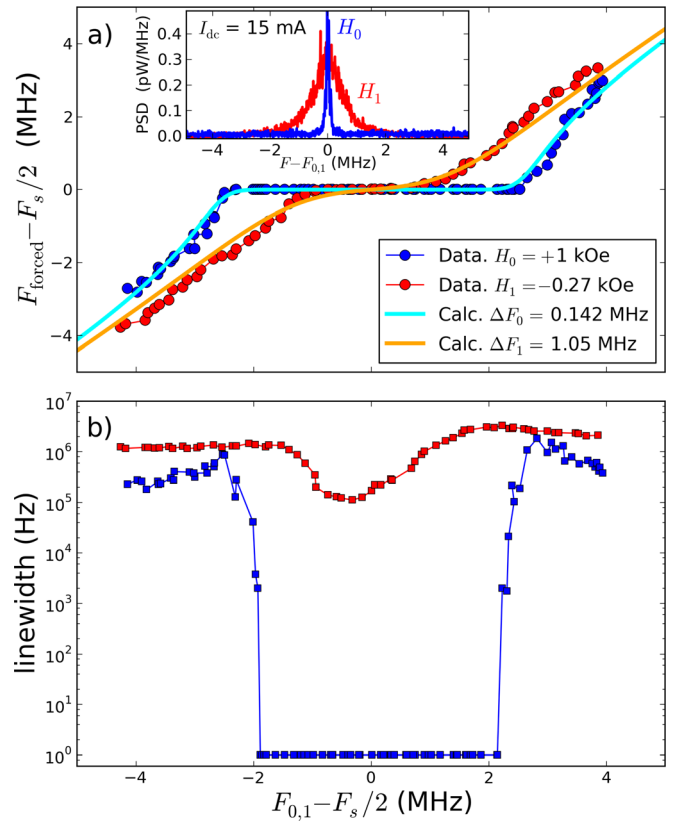


FIG. 4. (a) Variation of the frequency mismatch $F_{\text{forced}} - F_s/2$ as a function of the detuning $F_{0,1} - F_s/2$ at $H_0 = +1$ kOe (blue dots) and $H_1 = -0.27$ kOe (red dots). The external source amplitude is set to $h_{\text{rf}} = 6.3$ Oe. Continuous lines are fits using Eq. (5) of Ref. 27 yielding a coupling strength $\varepsilon = 2.5$ MHz. The inset shows the emission spectra at H_0 and H_1 in the free running regime. (b) Dependence of the emission linewidth on the frequency detuning at H_0 and H_1 .

the phase-locked regime, since its improvement with respect to the free running case drops from a factor 10^5 to only 10. The influence of phase fluctuations on the frequency mismatch has been modeled by Eq. (5) of Ref. 27 (see continuous lines in Fig. 4(a)). Using the measured linewidths ΔF_0 and ΔF_1 in this equation, the only fitting parameter is the coupling strength of the external microwave source to the oscillator (equal to half the locking range in the case of zero fluctuations), which is found to be $\varepsilon = 2.5$ MHz both at H_0 and H_1 .

In conclusion, we have shown that the microwave signal generated by a STNO based on coupled vortices can be efficiently synchronized to an external microwave field. The relative locking range indeed exceeds 10% for small drive amplitudes ($h_{\text{rf}} \approx 5$ Oe) and the auto-oscillation signal acquires the spectral purity of the source, corresponding to an improvement of its coherency by a factor greater than 10^5 . Moreover, this perfect phase-locking is robust, as it survives even when the external frequency deviates from the oscillator frequency by more than ten times its linewidth. We believe that the efficient synchronization of vortex-based STNOs to the microwave field is very promising for the idea of mutually coupling such oscillators through the dipolar interaction.⁴¹

This research was partly funded by the French ANR (Grant No. SPINNOVA ANR-11-NANO-0016) and the EU (FP7 Grant No. MOSAIC ICT-FP7-317950).

- ¹S. I. Kiselev, J. C. Sankey, I. N. Krivorotov, N. C. Emley, R. J. Schoelkopf, R. A. Buhrman, and D. C. Ralph, *Nature* **425**, 380 (2003).
- ²W. H. Rippard, M. R. Pufall, S. Kaka, S. E. Russek, and T. J. Silva, *Phys. Rev. Lett.* **92**, 027201 (2004).
- ³D. Houssameddine, U. Ebels, B. Delat, B. Rodmacq, I. Firastrau, F. Ponthenier, M. Brunet, C. Thirion, J.-P. Michel, L. Prejbeanu-Buda, M.-C. Cyrille, O. Redon, and B. Dieny, *Nature Mater.* **6**, 447 (2007).
- ⁴S. Bonetti, P. Muduli, F. Mancoff, and J. Åkerman, *Appl. Phys. Lett.* **94**, 102507 (2009).
- ⁵A. A. Tulapurkar, Y. Suzuki, A. Fukushima, H. Kubota, H. Maehara, K. Tsunekawa, D. D. Djayaprawira, N. Watanabe, and S. Yuasa, *Nature* **438**, 339 (2005).
- ⁶J. Zhu, J. A. Katine, G. E. Rowlands, Y.-J. Chen, Z. Duan, J. G. Alzate, P. Upadhyaya, J. Langer, P. K. Amiri, K. L. Wang, and I. N. Krivorotov, *Phys. Rev. Lett.* **108**, 197203 (2012).
- ⁷P. K. Muduli, Y. Pogoryelov, S. Bonetti, G. Consolo, F. Mancoff, and J. Åkerman, *Phys. Rev. B* **81**, 140408 (2010).
- ⁸Y. Pogoryelov, P. K. Muduli, S. Bonetti, E. Iacocca, F. Mancoff, and J. Åkerman, *Appl. Phys. Lett.* **98**, 192501 (2011).
- ⁹K. Mizushima, K. Kudo, T. Nagasawa, and R. Sato, *J. Appl. Phys.* **107**, 063904 (2010).
- ¹⁰J.-G. Zhu and Y. Wang, *IEEE Trans. Magn.* **46**, 751 (2010).
- ¹¹V. S. Pribiag, I. N. Krivorotov, G. D. Fuchs, P. M. Braganca, O. Ozatay, J. C. Sankey, D. C. Ralph, and R. A. Buhrman, *Nat. Phys.* **3**, 498 (2007).
- ¹²Q. Mistral, M. van Kampen, G. Hrkac, J.-V. Kim, T. Devolder, P. Crozat, C. Chappert, L. Lagae, and T. Schrefl, *Phys. Rev. Lett.* **100**, 257201 (2008).
- ¹³K. Y. Guslienko, *J. Nanosci. Nanotechnol.* **8**, 2745 (2008).
- ¹⁴A. Dussaux, B. Georges, J. Grollier, V. Cros, A. Khvalkovskiy, A. Fukushima, M. Konoto, H. Kubota, K. Yakushiji, S. Yuasa, K. Zvezdin, K. Ando, and A. Fert, *Nat. Commun.* **1**, 8 (2010).
- ¹⁵N. Locatelli, V. V. Naletov, J. Grollier, G. de Loubens, V. Cros, C. Deranlot, C. Ulysse, G. Faini, O. Klein, and A. Fert, *Appl. Phys. Lett.* **98**, 062501 (2011).
- ¹⁶A. Slavin and V. Tiberkevich, *IEEE Trans. Magn.* **45**, 1875 (2009).
- ¹⁷T. Shibata, R. Zhang, S. Levitan, D. Nikonov, and G. Bourianoff, in *Proceedings of 13th International Workshop on Cellular Nanoscale Networks and Their Applications (CNNA)* (2012), pp. 1–5.
- ¹⁸S. Kaka, M. R. Pufall, W. H. Rippard, T. J. Silva, S. E. Russek, and J. A. Katine, *Nature (London)* **437**, 389 (2005).
- ¹⁹F. B. Mancoff, N. D. Rizzo, B. N. Engel, and S. Tehrani, *Nature (London)* **437**, 393 (2005).
- ²⁰S. Sani, J. Persson, S. Mohseni, Y. Pogoryelov, P. Muduli, A. Eklund, G. Malm, M. Kil, A. Dmitriev, and J. Åkerman, *Nat. Commun.* **4**, 2731 (2013).
- ²¹A. Ruotolo, V. Cros, B. Georges, A. Dussaux, J. Grollier, C. Deranlot, R. Guillemet, K. Bouzehouane, S. Fusil, and A. Fert, *Nat. Nanotechnol.* **4**, 528 (2009).
- ²²A. N. Slavin and V. S. Tiberkevich, *Phys. Rev. B* **72**, 092407 (2005).
- ²³J. Grollier, V. Cros, and A. Fert, *Phys. Rev. B* **73**, 060409 (2006).
- ²⁴A. D. Belanovsky, N. Locatelli, P. N. Skirdkov, F. A. Araujo, J. Grollier, K. A. Zvezdin, V. Cros, and A. K. Zvezdin, *Phys. Rev. B* **85**, 100409 (2012).
- ²⁵S. Erokhin and D. Berkov, e-print [arXiv:1302.0659](https://arxiv.org/abs/1302.0659).
- ²⁶W. H. Rippard, M. R. Pufall, S. Kaka, T. J. Silva, S. E. Russek, and J. A. Katine, *Phys. Rev. Lett.* **95**, 067203 (2005).
- ²⁷B. Georges, J. Grollier, M. Darques, V. Cros, C. Deranlot, B. Marciilhac, G. Faini, and A. Fert, *Phys. Rev. Lett.* **101**, 017201 (2008).
- ²⁸M. Quinsat, J. F. Sierra, I. Firastrau, V. Tiberkevich, A. Slavin, D. Gusakova, L. D. Buda-Prejbeanu, M. Zarudniev, J.-P. Michel, U. Ebels, B. Dieny, M.-C. Cyrille, J. A. Katine, D. Mauri, and A. Zeltser, *Appl. Phys. Lett.* **98**, 182503 (2011).
- ²⁹A. Dussaux, A. V. Khvalkovskiy, J. Grollier, V. Cros, A. Fukushima, M. Konoto, H. Kubota, K. Yakushiji, S. Yuasa, K. Ando, and A. Fert, *Appl. Phys. Lett.* **98**, 132506 (2011).
- ³⁰S. Urazhdin, P. Tabor, V. Tiberkevich, and A. Slavin, *Phys. Rev. Lett.* **105**, 104101 (2010).
- ³¹A. Hamadeh, G. de Loubens, V. V. Naletov, J. Grollier, C. Ulysse, V. Cros, and O. Klein, *Phys. Rev. B* **85**, 140408 (2012).
- ³²V. V. Naletov, G. de Loubens, G. Albuquerque, S. Borlenghi, V. Cros, G. Faini, J. Grollier, H. Hurdequint, N. Locatelli, B. Pigeau, A. N. Slavin, V. S. Tiberkevich, C. Ulysse, T. Valet, and O. Klein, *Phys. Rev. B* **84**, 224423 (2011).
- ³³V. Sluka, A. Kákay, A. M. Deac, D. E. Bürgler, R. Hertel, and C. M. Schneider, *Phys. Rev. B* **86**, 214422 (2012).
- ³⁴P. N. Skirdkov, A. D. Belanovsky, K. A. Zvezdin, A. K. Zvezdin, N. Locatelli, J. Grollier, and V. Cros, *Spin* **02**, 1250005 (2012).
- ³⁵A. Hamadeh, G. de Loubens, O. Klein, V. Naletov, N. Locatelli, R. Lebrun, J. Grollier, and V. Cros, e-print [arXiv:1310.4913](https://arxiv.org/abs/1310.4913).
- ³⁶The output power from the synthesizer injected into the microwave antenna is set to $P = 0$ dBm.
- ³⁷A. V. Khvalkovskiy, J. Grollier, A. Dussaux, K. A. Zvezdin, and V. Cros, *Phys. Rev. B* **80**, 140401 (2009).
- ³⁸E. Grimaldi, A. Dussaux, P. Bortolotti, J. Grollier, G. Pilllet, A. Fukushima, H. Kubota, K. Yakushiji, S. Yuasa, and V. Cros, e-print [arXiv:1311.6299](https://arxiv.org/abs/1311.6299).
- ³⁹This change of linewidth is due to the influence of a lower frequency over-damped mode.³⁵
- ⁴⁰In these measurements, $h_{rf} = 6.3$ Oe and I_{dc} is varied from 14.6 mA to 15.6 mA. At H_0 , F_0 varies from 584 MHz to 592 MHz and F_s is fixed to 1175 MHz. At H_1 , F_1 varies from 681 MHz to 689 MHz and F_s is fixed to 1370 MHz.
- ⁴¹A. D. Belanovsky, N. Locatelli, P. N. Skirdkov, F. Abreu Araujo, K. A. Zvezdin, J. Grollier, V. Cros, and A. K. Zvezdin, *Appl. Phys. Lett.* **103**, 122405 (2013).